Biogeosciences Discuss., 7, 7091–7130, 2010
www.biogeosciences-discuss.net/7/7091/2010/
doi:10.5194/bgd-7-7091-2010

Biogeosciences Discussions

Accumulation of DOC in Low Phosphate Low Chlorophyll (LPLC) area: is it related to higher production under high N:P ratio?

R. Mauriac, T. Moutin, and M. Baklouti

(INSU-CNRS, Laboratoire d'Océanographie Physique et Biogéochimique, UMR 6535, Centre d'Océanologie de Marseille, Université de la Mediterranée, France)

Received: 29 July 2010 – Accepted: 31 August 2010 – Published: 23 September 2010

Correspondence to: R. Mauriac (romain.mauriac@univmed.fr)

Published by Copernicus Publications on behalf of the European Geosciences Union.

Abstract

The biogeochemistry of carbon and nutrients (N, P) in the surface layer of the ocean strongly depends on the interaction between C, N and P at the cell level and at the population level where interaction between primary producers (phytoplankton) and remineralizers (heterotrophic bacteria) impact the overall stock and dynamics of organic carbon. To understand these interactions in the surface layer of the Mediterranean Sea, we implemented, using Eco3M, a multi-element, steady state, mechanistic model. This cell-based model intend to represent the growth of phytoplankton and heterotrophic bacteria under various amount of nutrients. As a results, it displays the expected biogeochemical characteristics of the system and give us insight on the expected interaction between phytoplankton and heterotrophic bacteria both in term of competition for inorganic nutrients and in term of commensalism for organic carbon. In this study, we found a good quantitative agreement between model results and literrature data for stocks and fluxes of the western Mediterranean basin. In addition, for phytoplankton we show how the uncoupling between carbon production and growth could impact the overall DOC dynamic and based on these results, we proposed a new explanantion for the observed DOC accumulation in the surface layer of the Mediterranean Sea.

1 Introduction

During summer, the surface layer of the Meditteranean Sea is a low phosphate low chlorophyll system (Moutin et al., 2008). The high nitrate to phosphate ratio observed below the euphtoic zone (Krom et al., 1991) and the significant response of primary and bacterial production in bioassay experiments have suggested that both phytoplankton and heterotrophic bacteria are P-limited or NP-colimited (Thingstad et al., 1998, 2005). Unfortunately, inorganic nutrients concentrations are often close to or below the detection limit in this layer and elemental content of osmotrophs is rarely quantified directly on board. This makes the understanding of the coupling between carbon, nutrients and

BGD
7, 7091–7130, 2010

growth at the cell level difficult to assess. On short time scales, the observed response in bioassay experiments is likely to be a relatively complex phenomenon involving cell physiology for uptake, as well as, storage of limiting and near limiting resources. This is regarded as a key issue when trying to understand the coupling between nutrient and carbon in the eupohtic zone. To overcome this issue, theoretical mechanistic models provide a good alternative to in situ measurements. A Numerical model based on P-limitation of both bacterial and phytoplanktonic growth has sucessfully described qualitatively some of the observed features of the surface water of the Mediterranean Sea (Thingstad, 2005). However, for heterotrophic bacteria, enrichment in both organic carbon and nutrients systematically leads to a stronger response compared to experiments with nutrients alone (Wambeke et al., 2002). This means that interaction between heterotrophic bacteria and phytoplankton is probably more complex than simple competition for inorganic nutrients and that the organic carbon production rate and the lability of the different available carbon sources may also play a role in the observed DOC dynamics. In this study, we investigate a simple steady state mechanistic model that includes both competition for inorganic nutrients and commensalism (through DOC exudation and remineralization) between picophytoplankton and heterotrophic bacteria. Our results suggest that although the system appears balance or net hetrotrophic during summer, the ratio of inorganic nitrogen to inorganic phosphate could have an impact on the observed DOC accumulation in the surface layer of LPLC areas over seasonal time sclaes.

2 Model description

2.1 Overview

During summer, the offshore surface water of the Mediterranean Sea is characterized by low levels of production, small organisms and stable stratification. In addition, variation in cellular abundance of phytoplankton is relatively small suggesting a state of

BGD
7, 7091–7130, 2010

particular equilibrium for this functionnal group (Magazzu and Decembrini, 1995). For heterotrophic bacteria, the close coupling between bacterial production and predation by higher trophic level, suggests a similar pattern (Christaki et al., 2001). Based on these considerations, we assumed a constant cell abundance for both groups. During this period of stable stratification, the system relies mostly on regenerated nutrients due to internal recycling of organic matter (Moutin and Raimbault, 2002). Hence, we assumed that the system could be assimilated to a steady state system where loss of nutrients is compensated by remineralization of organic compounds, making dissolved organic nitrogen (DON) and phosphate (DOP) implicit in our model. The conceptual model (Fig. 1) that comes from our steady state assumptions includes two living compartments (picophytoplankton and heterotrophic bacteria), two inorganic compartments (N and P) and three detritic compartments that supply the bacterial carbon demand (BCD). DOC production in the model is the result of two distinct processes. It is either supplied by exudation of carbon by phytoplankton (photosynthetic extracelullar release (PER)) or via grazing and mortality. The DOC supplied through grazing and mortality represented 50% of phytoplankton and bacterial mortality as suggested by Hagstrom et al. (1988). The other half is supposed to be transferred to higher trophic level. In the model, 40% of DOC orginating from grazing and mortality is assumed to be a semi refractory form (SRDOC) and 10% is present as a labile form (LDOC). The fractionation between LDOC and SRDOC is intended to represent the release of compounds during cell lysis processes with different lability. Although our choice is quite arbitrary, it is close to values concerning the fraction of total DOC that is considered to be labile (Sondergaard and Middelboe, 1995).

2.1.1 State equations

Phytoplankton

$$\frac{d\phi}{dt} = f_{\phi}^{\mu}\ \phi - f_{\phi}^{\mu}\ \phi = 0 \qquad (1)$$

BGD
7, 7091–7130, 2010

$$\frac{d\phi_C}{dt} = f_{nr}^{PP} \; f_{\phi}^{Q_C} \; \phi_C - f_{\phi}^{resp} \; \phi_C - f_{\phi}^{\mu} \; \phi_C \quad (2)$$

$$\frac{d\phi_N}{dt} = f_{\phi}^{upt_N} \; f_{\phi}^{Q_N} \; \phi_N - f_{\phi}^{\mu} \; \phi_N \quad (3)$$

$$\frac{d\phi_P}{dt} = f_{\phi}^{upt_P} \; f_{\phi}^{Q_P} \; \phi_P - f_{\phi}^{\mu} \; \phi_P \quad (4)$$

$$\frac{d\phi_{Chl}}{dt} = f^{Chl} - f_{\phi}^{\mu} \; \phi_{Chl} \quad (5)$$

Bacteria

$$\frac{d\beta}{dt} = f_{\beta}^{\mu} \; \beta - f_{\beta}^{\mu} \; \beta = 0 \quad (6)$$

$$\frac{d\beta_C}{dt} = (f_{\beta}^{upt_{LDOC}} + f_{\beta}^{upt_{SLDOC}} + f_{\beta}^{upt_{SRDOC}}) \; f_{\beta}^{Q_C} \; \beta_C - f_{\beta}^{resp} \; \beta_C - f_{\beta}^{\mu} \; \beta_C \quad (7)$$

$$\frac{d\beta_N}{dt} = f_{\beta}^{upt_N} \; f_{\beta}^{Q_N} \; \beta_N - f_{\beta}^{\mu} \; \beta_N \quad (8)$$

$$\frac{d\beta_P}{dt} = f_{\beta}^{upt_P} \; f_{\beta}^{Q_P} \; \beta_P - f_{\beta}^{\mu} \; \beta_P \quad (9)$$

Dissolved organic carbon

$$\frac{dLDOC}{dt} = 0.1 \; (f_{\phi}^{\mu} \; \phi_C + f_{\beta}^{\mu} \; \beta_C) - f_{\beta}^{upt_{LDOC}} \; f_{\beta}^{Q_C} \; \beta_C \quad (10)$$

$$\frac{dSLDOC}{dt} = f_{nr}^{PP} \; (1 - f_{\phi}^{Q_C}) \; \phi_C - f_{\beta}^{upt_{SLDOC}} \; f_{\beta}^{Q_C} \; \beta_C \quad (11)$$

$$\frac{dSRDOC}{dt} = 0.4 \; (f_{\phi}^{\mu} \; \phi_C + f_{\beta}^{\mu}) \; \beta_C - f_{\beta}^{upt_{SRDOC}} \; f_{\beta}^{Q_C} \; \beta_C \quad (12)$$

BGD
7, 7091–7130, 2010

Nutrients

$$\frac{dN}{dt} = f_{\phi}^{\mu}\ \phi_N + f_{\beta}^{\mu}\ \beta_N - f_{\beta}^{upt_N}\ f_{\beta}^{Q_N}\ \beta_N - f_{\phi}^{upt_N}\ f_{\phi}^{Q_N}\ \phi_N \quad (13)$$

$$\frac{dP}{dt} = f_{\phi}^{\mu}\ \phi_P + f_{\beta}^{\mu}\ \beta_P - f_{\beta}^{upt_{PO_4}}\ f_{\beta}^{Q_P}\ \beta_P - f_{\phi}^{upt_{PO_4}}\ f_{\phi}^{Q_P}\ \phi_P \quad (14)$$

Our system is mathematically described using 14 state variables (Table 1 and Eqs. 1–14) and and 4 biogeochemical processes, namely growth, nutrient uptake, primary production and respiration (cf. Sect. 2.2–2.5). Bacterial and phytoplanktonic biomass are described in term of cellular abundance and C,N,P biomass and an additional state variable representing chlorophyll biomass is present as part of the mechanistic description of the photosyntheic processes (Sect. 2.4). For phytoplankton we assume that the population was composed solely of synechococcus cells, a genus known to dominate in the surface layer of the Mediterranean Sea during the summer period (Vaulot et al., 1996).

2.2 Intracellular quota and growth

The model is based on the assumption that there are a minimum (Q^{min}) and maximum (Q^{max}) intracellular content for each element (C, N, P). Q^{min} can be interpreted as the amount of element used in cellular structure and machinery and everything else can be seen as storage for future growth. Since Droop and his work on vitamin B12 (Droop, 1968), this concept has been widely used, especially to simulate change in organisms' stoichiometry (Klausmeier et al., 2008). We therefore used the classical Droop formulation (Eq.15) combined with the Leibig's law of the minimum to describe growth rate.

$$f^{\mu} = \bar{\mu}\ \min\left(1 - \frac{Q_X^{min}}{Q_X}\right) \quad (15)$$

BGD
7, 7091–7130, 2010

In this formulation, Q_X^{min} represents the minimum cell content for a given element X, Q_X the actual cell content and $\bar{\mu}$ the maximum theoretical growth rate of the organism. It should be noted that using explicit maximum intracelullar quota implies that $\bar{\mu}$ is never achieved. The maximum achievable growth rate ($\hat{\mu}$) is conditioned by the Q^{max} values of the element for which the organism possess the smallest storage capacity. Since we assumed that for every element Q^{max} is 2.5 times greater than Q^{min}, the maximum achievable growth rate $\hat{\mu}$ is equal to $0.6\,\bar{\mu}$. The value of 2.5 was chosen in order to stay within a reasonable range compared to literature data. Also, we assumed that $\bar{\mu}$ is the same regardless of the element or the organisms considered. We can suspect these assumptions are not always verified (Goldman and McCarthy, 1978; Terry et al., 1985), but to keep the model as simple as possible, we have used them in our simulations. For phytoplankton and bacteria, maximum growth rate $\bar{\mu}$ is set to $2\,d^{-1}$ thus $\hat{\mu}$ is equal to 1.2 d.

The minimum P content for bacteria is set to $0.50\,fgP\,cell^{-1}$ (Table 2) which is close to values found for aquatic bacteria (Fagerbakke et al., 1996; Gundersen et al., 2002; Lovdal et al., 2008). Using an optimal C:N:P ratio of 50:10:1 (Fagerbakke et al., 1996), minimum C content is $9.68\,fgC\,cell^{-1}$ which seems acceptable for small oceanic bacteria (Fukuda et al., 1998; Gundersen et al., 2002). The minimum nitrogen content of $2.26\,fgN\,cell^{-1}$, resulting from the optimal ratio selected, is also close to published values for oceanic bacteria (Fukuda et al., 1998). For phytoplankton, the minimum P content is $2\,fgP\,cell^{-1}$. It is in the range of values found in the literature using both direct and indirect measurements (Ikeya et al., 1997; Heldal et al., 2003; Bertilsson et al., 2003). Using the redfield ratio as the optimal ratio (C:N:P 106:16:1), the minimum carbon and nitrogen content in phytoplanktonic cells are repspectively $82\,fgC\,cell^{-1}$ and $14.5\,fgN\,cell^{-1}$.

BGD
7, 7091–7130, 2010

2.3 Uptake of carbon and nutrients

To describe maximum gross uptake rate of nutrients and dissolved organic carbon, the Michaelis-Menten relationship was chosen for its simplicity (Eq. 16). A feedback from internal cellular status to mediate the net uptake rate is in the form of a quota function (Eq. 17) (Lehman et al., 1975).

$$f_X^{\text{upt}} = V_X^{\max} \frac{[X]}{[X] + K_X} f^{Q_X} \tag{16}$$

$$f^{Q_X} = \frac{Q_X^{\max} - Q_X}{Q_X^{\max} - Q_X^{\min}} \tag{17}$$

$V_X^{\max}$ and K_X are assumed constant in the model and represent the uptake parameters one would obtain from nutrient starved organisms (e.g. maximum potential uptake rate). This maximum potential uptake rate is associated with a maximum theoretical affinity α, which represents the volume of water cleared for nutrients per unit of biomass per hour. For a spherical cell, and assuming that all molecules reaching the cell through molecular diffusion are captured, the theoretical expression for α is (Thingstad and Rassoulzadegan, 1999):

$$\alpha = \frac{3D}{\sigma r^2} \tag{18}$$

Here, D is the diffusion constant for phosphate, σ is the internal phosphate concentration (mol μm^{-3}), and r is the cell radius. Eq. 18 can be rearranged as follow:

$$\alpha = \frac{4 \ \pi \ D \ r}{p} \tag{19}$$

In Eq. 19, p represent the intracellular elemental content (mol cell^{-1}) and thus differs from σ. Finally, The maximum affinity constant could also be obtained using the

BGD
7, 7091–7130, 2010

relationship from Healey (1980):

$$\alpha = \frac{V^X}{K_X \ [\text{cell}] \ p} \tag{20}$$

In Eq. 20, V^X is the maximum uptake rate obtain at the population level ($\text{mol}\,\text{m}^{-3}\,\text{s}^{-1}$) and [cell], the cellular abundance ($\text{cell}\,\text{m}^{-3}$). Using Eq. 19 and Eq. 20 we obtain the following relationship:

$$V_X^{\max} = \frac{V^X}{[\text{cell}]} \tag{21}$$

$$\frac{V_X^{\max}}{K_X} = 4\,\pi\,D\,r \tag{22}$$

In Eq. 22, the assumption is that under extremely low nutrient concentrations, the slope of the Michaelis Menten relationship is equal to the diffusion rate of the molecules. In this study, D was set to $10^{-9}\,\text{m}^2\,\text{s}^{-1}$, an intermediate value commonly used for ions in seawater (Yuan-Hui and Gregory, 1974), and r was set to 0.5 and 0.18 µm for phytoplankton and bacteria respectively (Table 2). Based on our size considerations, on the Michaelis Menten parameters present in the literature (Vadstein and Olsen, 1989; Ikeya et al., 1997; Fu et al., 2006) and on the fact that we wanted bacteria to be more competitive than phytoplankton in terms of nutrient aquisition. We obtained the uptake parameters displayed in Table 2. In addition, since we did not see any reason for assuming differences in the maximum gross uptake of both nutrients, the model assumes that the uptake parameters are identical for both P and N, assuming that the Michaelis Menten relationship for N under N depleted condition is similar to the Michaelis Menten relationship for P under P depleted condition. For DOC uptake, we set $V_X^{\max}$ and K_X values arbitrarily to obtain maximum affinity constants one and two orders of magnitude lower than for inorganic nutrients for LDOC and SLDOC & SRDOC respectively. It allows us to take into account the larger size and thus lower diffusion rate of these

BGD
7, 7091–7130, 2010

molecules as well as the longer hydrolyse step require before bacteria can assimilate these compounds. To take into account the fact that bacteria may not grow at the same rate depending on the carbon source (Middelboe and Sondergaard, 1993), we associated with each DOC source a specific growth yield (Sect. 2.5). The most reliable DOC source for bacterial growth being LDOC followed by SLDOC and SRDOC (Table 5).

2.4 Photosynthesis and chlorophyll production

The model uses a mechanistic formulation for photosynthesis and chlorophyll production. The photosynthesis model is based on the idea that the quantum yield of carbon fixation is proportional to the probability of photosystem II being open and was originaly presented by Han (2002). The chlorophyll model relies on the fact that the rate at which chlorophyll is produced depends on the nitrogen status of the cell (Baklouti et al., 2006a). A thorough investigation of the present mathematical description can be found in the the two papers by Baklouti et al. (2006a,b). This formulation was chosen for its mechanistic approach and the fact that all parameters are measurable. One modification to the chlorophyll synthesis model was made concerning the rate at which chlorophyll is produced. We arbitrarily chose to scale the production rate to the maximum growth rate to allow chlorophyll synthesis in the case where intracellular N content is greater than $Q_{\mathrm{N}}^{\mathrm{min}}$ but uptake rate is zero.

$$f_{nr}^{\mathrm{PP}} = \frac{\phi_{\mathrm{max}}^{\mathrm{C}} \;\; \bar{a}^{*} \;\; E \;\; Q_{\mathrm{Chl/C}}^{i}}{1+\sigma_{\mathrm{PSII}} \;\; E \;\; \tau+(k_d^H/k_r) \;\; (\sigma_{\mathrm{PSII}} \;\; E)^2 \;\; \tau} \tag{23}$$

$$f^{\mathrm{PChl}} = \frac{\bar{\mu}_{\mathrm{phi}} \;\; (Q_{\mathrm{Chl/N}}^{i})_{\mathrm{max}} \;\; f_{nr}^{\mathrm{PP}}}{\bar{a}^{*} \;\; \phi_{\mathrm{max}}^{C} \;\; Q_{\mathrm{Chl/C}}^{i} \;\; E} \;\; \frac{1-Q_{\mathrm{Chl/N}}^{i}/(Q_{\mathrm{Chl/N}}^{i})_{\mathrm{max}}}{(1-Q_{\mathrm{Chl/N}}^{i}/(Q_{\mathrm{Chl/N}}^{i})_{\mathrm{max}})+0.05} \tag{24}$$

In Eq. 23 and 24, ϕ_{max}^{C} represents the maximum quantum yield for carbon fixation, $\bar{a}^{*}$, the mean Chl a specific absorption coefficient, E, the irradiance, $Q_{\mathrm{Chl/C}}^{i}$ the chlorophyll

BGD
7, 7091–7130, 2010

to carbon ratio,σ_{PSII}, the PSII cross section, τ, the electron turnover time, k_d^H, the PSII damage rate, k_r, the PSII repair rate and $(Q^j_{Chl/N})_{max}$ the maximum chlorophyll to nitrogen ratio. Parameter were chosen to stay within the range of published values for phytoplankton (Yentsch and Vaccaro, 1958; Claustre et al., 2005)

2.5 Respiration rate

In the model, respiration for phytoplankton is described by a "maintenance" cost associated with the excess carbon present in osmotrophic cells (see Thingstad (1987) for more detailed concernning the term "maintenance").

$$f_{\phi}^{resp} = (Q_C - Q_C^{min})\ \ \omega_4 \tag{25}$$

One aspect is that respiration rate will increase with increasing carbon intracellular content and thus conveys the idea that respiration rate may be higher during the day, a feature that has been observed in natural communities (Weger et al., 1989). For heterotrophic bacteria respiration rate is a combination of a "maintenance" cost and a cost for DOC aquisition:

$$f_{\beta}^{resp} = (Q_C - Q_{vC}^{min})\ \ \omega_4 + (1-\omega_1) f_{\beta}^{upt_{LDOC}} + (1-\omega_2) f_{\beta}^{upt_{SLDOC}} + (1-\omega_3) f_{\beta}^{upt_{SRDOC}} \tag{26}$$

This choice to describe respiration rate was motivated by the fact that respiration rate may vary with DOC quality and it allows two type of carbon limitation, either limitation by availability (when DOC ressource is low) or limitation by lability (when DOC aquisition is costly) both cases resulting in a low bacterial growth rate (Thingstad and Lignell, 1997).

BGD
7, 7091–7130, 2010

3 Simulations set up

To describe the day/night cycle, the model was run with a given light regime described by the following equation:

$$E = E_{max} \; e^{1.5 \; \cos(2\pi \; (t/(24 \; 3600))-1)} \quad (27)$$

Where E_{max} represents the irradiance at noon under the surface (Wm^{-2}) and t the time in seconds. Since we set the mortality rate equal to the cellular growth rate at all time, cellular abundance is always constant and was fixed to $5\,10^8$ cell l^{-1} and $2.5\,10^7$ cell l^{-1} for bacteria and phytoplankton respectively. This choice was made in order to obtain similar carbon biomass for both functionnal groups and we checked to stay within a reasonnable range of litterature values for bacteria (Robarts et al., 1996; Lemee et al., 2002; Tanaka and Rassoulzadegan, 2004) and phytoplankton (Wambeke et al., 2001; Christaki et al., 2002; Tanaka and Rassoulzadegan, 2002; Siokou-Frangou et al., 2010) in the western Mediterranean bassin. At the start of each simulations, organisms are at their minimum intracellular content for all elements, Chl:C is set to 0.25 gChl $molC^{-1}$ and DOC compartments are set to zero. Each simulations were run for 100 days with a fix amount of nitrogen and phosphate until a steady state regime was reached.

4 Results

The best way to interpret the results of our simulations is to consider that the model solves the mass balance equations for given growth conditions. Given a total amount of nitrogen (TN) and phosphate (TP) arbitrarily distributed, the model calculates the distribution of N and P among the different compartments and displays the biogeochemical fluxes and concentrations required in order to maintain a given population under a fix amount of nutrients (N and P). The carbon budget in the model is then infered from the balance between carbon production through primary production, grazing or mortality

BGD
7, 7091–7130, 2010

and carbon respiration which depends on the cellular C-content and on the efficiency at which heterotrophic bacteria assimilate DOC.

Environmental conditions, growth and nutrient uptake

We ran the model for a wide range of total nitrogen (TN) and total phosphate (TP) values, from 160 to 640 nM for TN and from 10 to 40 nM for TP (Fig. 2a). The resulting TN:TP ratio range from 5 to 60 and represents P limited as well as N-limited environment (Fig. 3a, b). Within the range of TN and TP used in this study, inorganic nutrient concentrations range from 0 to 15 nM and from 0 to 370 nM for phosphate and nitrogen respectively (Fig. 2b). Under these conditions, phytoplankton growth rate ranges between 0 and 0.53 div d^{-1} (Fig. 3a) and bacterial growth rate ranges between 0 and 0.5 div d^{-1} (Fig. 3b). For phytoplankton, the maximum growth rate is found when nutrient concentrations are higher than 0.09 nM and 2 nM for phosphate and nitrogen respectively. In contrast, for heterotrophic bacteria the maximum growth rate is found for low P concentrations (0.06 to 0.08 nM) associated with relatively high N concentrations (>10 nM).

This particular feature for heterotrophic bacterial growth is the result of a higher affinity for phosphate associated with high DOC availability (Fig. 7) which in turn results from a high DOC exudation rate by phytoplankton (Fig. 5d). Nutrient uptake rates ranged from 0 to 6 nmol l^{-1} d^{-1} for P (Fig. 4b) and from 0 to 115 nmol l^{-1} d^{-1} for N (Fig. 4a). Uptake of both elements show non-linear patterns with respect to environmental conditions. Uptake of inorganic nitrogen is maximum where bacterial growth rate is high. Under these conditions, the fraction of N uptake attributed to phytoplankton is below 25 % (data not shown) and total inorganic N uptake is mainly attributable to heterotrophic bacteria. In the simulations where both phytoplankton and bacteria are P-limited (10 nM<TP<15 nM), an increase in N uptake is observed with increasing P availability (Fig. 4a) and an increasing fraction of the uptake is attributable to phytoplankton (from 17 to 25% (data not shown)). For TP values above 15 nM, N uptake rate tends to decrease (Fig. 4a) and this is mainly due to a decrease of bacterial

BGD
7, 7091–7130, 2010

uptake caused by an increasing C-limitation of heterotrophic bacterial growth (Fig. 3b). Concerning P uptake the pattern is slightly different. Two maximum uptake rates are found (Fig. 4b). The first one is found for TP values between 13 and 15 nM and is associated with the high N uptake rate described above and thus is mainly attributable to heterotrophic bacteria (85% of total P-uptake (data not shown). The second maximum is observed under low N conditions (TN<200 nM) and relatively high P conditions (TP>25 nM). Under these conditions, the fraction of P uptake attributed to phytoplankton is higher and represents 20 to 40% of total P uptake (data not shown). We thus obtained similar P uptake rates for two completely different settings where phytoplankton could either be P or N limited and heterotrophic bacteria P or C limited. In Fig. 4d turnover of phosphate, which represents the inorganic P concentration divided by the P uptake rate at steady state, ranges from less than 0.25 h to more than 50 h and seems to increase linearly with inorganic phosphate concentrations. In contrast, it is poorly correlated to the P uptake rate, despite a slight shift under low N conditions where P uptake rate is maximum. This highlights the fact that under steady state conditions, turnover time of phosphorus is much more sensitive to a change in nutrient concentrations than to a change in uptake rate. Finally, The uncoupling of N and P uptake in the model is highlighted by the wide range of N:P ratio associated with a given P uptake rate (Fig. 4c). Globally, the N:P ratio for nutrient uptake predicted by the model ranges from 6 to 24 and generally increases with increasing TN:TP ratio (Fig. 2a and Fig. 4c).

4.1 Carbon Budget: Primary Production vs Bacterial Production

From the producers end (i.e. phytoplankton), gross primary production range from 0.3 to 0.9 µmol l^{-1} d^{-1} (Fig. 5a). The highest rate for GPP is found for low TP values (where phytoplankton growth is P-limited) and TN values above (250 nM). This increase in GPP with decreasing P availability is counterintuitive and is mainly the results of the higher chlorophyll content found in this type of simulation (Fig. 5c). In fact, when growth is P-limited and when inorganic N is abundant, nitrogen cell content of phytoplankton increases until it reaches Q_N^{max}. Since maximum chlorophyll content is scaled to the N

BGD
7, 7091–7130, 2010

content of the cell, Chlorophyll concentration is maximum and so is GPP. However due to the P-limitation of phytoplanktonic growth under low P environment, most of the carbon fixed during gross primary production is exuded as DOC (Fig. 5d) and fuelled the BCD (Fig. 6a) or accumulate as DOC (Fig. 7). In our model, phytoplankton exudation range from 21 to 72% of GPP and it increases with increasing oligotrophy. The balance between GPP, exudation and respiration of storage compounds results in a net primary production rate ranging from 0.015 to 0.12 µmolC l^{-1} d^{-1} (Fig. 5b). Net primary production in the model is equivalent to the specific growth rate (h^{-1}) of phytoplankton multiply by its carbon biomass. Thus increase in NPP is either the result of an increasing specific growth rate or of an increasing carbon intracellular content both of which tend to behave in opposite way. For example, under nutrient limited environment growth is limited by nutrients and growth rate decreases but, at the same time, carbon accumulates in the cell increasing the carbon biomass of the phytoplanktonic compartment. Thus similar net primary production rate could be found for different specific growth rate assuming that they are associated with different carbon intracellular content. From the consumers end (e.g. bacteria), the bacterial carbon demand (BCD) represent the total amount of DOC taken up by heterotrophic bacteria prior to respiration and ranges from 0.13 to 0.67 µmol l^{-1} d^{-1} (Fig. 6a). The amount of carbon respired integrates respiration of stored compounds as well as respiration due to change in DOC quality (Fig. 6c) and range from 0.1 to 0.55 µmol l^{-1} d^{-1}. The bacterial growth efficiency (BGE = $\frac{BP}{BR+BP}$) ranges between 0 and 41% (Fig. 6b). BGE decreases with increasing oligotrophy and this is the result of an increase of bacterial respiration which is more important than the increase in bacterial production. For example, over the same range of TP values from 16 to 12 nM and for similar TN values (480 nM), BP increase from 0.16 µmol l^{-1} d^{-1} (TP = 16 nM) to 0.24 µmol l^{-1} d^{-1} (TP = 12 nM) while bacterial respiration increases from 0.24 µmol l^{-1} d^{-1} to 0.42 µmol l^{-1} d^{-1} over the same range. Thus while BP increased by 50%, BR increases by 75% resulting in a overall decrease in BGE of about 10%. Under even lower TP concentrations, BP start to decrease while BR continue to increase resulting in an even lower BGE. However, BGE is only sensitive to nutrient limitation and

BGD
7, 7091–7130, 2010

seems more correlated to nutrient availability than to carbon availability. If we consider bacterial production (BP) which was assumed to be the growth rate of the organisms multiply by its carbon content, values range between 0.05 to 0.25 µmol l^{-1} d^{-1} (Fig. 6d). The overall results of the balance between carbon production and carbon respiration is the possible accumulation of DOC in the model. For most of our simulations, DOC does not accumulate and displays values close to zero which is consistent with the idea of balance carbon budget during the summer period. However in the case of low TP values and high TN values, the model predicts a net production of DOC which results in the accumulation 5 µM of DOC within the hundred days of our simulations. This result is of particular interest and highlight the ability of the model to produce more carbon than required under high N:P ratio compare to balance (16:1) or low N:P ratio. To which extent this result is relevant when trying to understand the accumulation of DOC in the surface layer of the Mediterranean Sea is discussed in the next section.

5 Discussion

In the surface layer of the ocean, understanding the interaction between heteotrophic bacteria and phytoplankton is a complex issue that involves competition in terms of inorganic nutrients and commensalism in terms of carbon. While some authors have focused on the competition for inorganic nutrients (Thingstad, 2005; Thingstad et al., 1997), others have focused on the balance between primary production and respiration (Anderson and Ducklow, 2001; Anderson and Turley, 2003). However, to our knowledge, none have tried to tackle both issues at the same time using a simple steady state model such as the one describe in this study. Combining a C-based model with a nutrient based model requires a framework in which all three elements can be coupled in a coherent manner. The use of cellular abundances and variable intracellular elemental contents combined with a Droop-like approach for growth appears as a relatively simple and straightforward description that allows the coupling of carbon and nutrients in living population using relatively realistic constraints. At the cell level, clear

BGD
7, 7091–7130, 2010

constraints in terms of biomass (using maximum and minimum intracellular content) and in terms of nutrient uptake (using size considerations and diffusion limitation) are very useful for the calibration of a model. Although this study is not a validation of the model in a strict sense, we can notice that the overall range of values displayed by the model, in term of N and P, are consistent with published data for the Mediterranean sea. For inorganic phosphate, due to the quantification limit of commonly used measurement techniques (50 nM), it is difficult to assess whether or not the concentrations displayed by the model are reasonnable. Nonetheless, in the literature, inorganic phosphate concentrations at the surface was suggested to lie somewhere between 0.1 and 5 nM during summer and the associated turnover times are of the order of a few hours (Thingstad et al., 1996; Moutin et al., 2002). These findings are reasonably close to our model values for phosphate (Fig. 2b and 4d). Since the Mediterranean sea is assume to be P-limited, few study have focus on the dynamic of the non-limiting elements such as inorganic nitrogen. In contrast to inorganic phosphate concentrations, a substantial amount of inorganic nitrogen can remain at the surface, especially in the eastern basin (Krom et al., 1992). The main consequence is that, in the surface layer, high N:P ratio could be expected and model results displaying more than 300 nM of inorganic N with close to zero nM of P may not be unreasonnable. In the Gulf of Lions (western basin), Diaz and Raimbault (2000) measured uptake rate (NH_4 + NO_3) close to our values, ranging from 50 to 100 nmol l^{-1} d^{-1} at the onset of the stratified period. Looking at our model results for N and P uptake (Fig. 4a and 4b), our size assumption combined with the cellular abundance selected for our simulations seems to give a satisfying first approximation of the expected nutrient fluxes for the western basin. Concerning cellular growth rate, values are in the range of reported values for osmotrophs in the oceans (Duhamel et al., 2007). Although the estimation of osmotrophs growth rate in oceanic environment is still subject to debate, it has been suggested that phytoplankton growth rate are well below their maximum growth rates and that values below 0.5 div d^{-1} are consistent with the existing knowledge on the relationship between elemental composition and physiological state in phytoplankton (Maranon, 2005). Our model seems to

BGD
7, 7091–7130, 2010

concur with such hypotheses at least for small phytoplankton in oligotrophic environment. In terms of growth limitation, model results are also quite consistant with what has been reported in the literature based on bioassays experiments. For heterotrophic bacteria positive response to P and C enrichement were observed (Wambeke et al., 2002) and for picophytoplankton, enrichement experiments show either P-limitation or NP-colimitation (Thingstad et al., 1998, 2005). However in our model, growth limitation by phosphate of both osmotrophic groups is restricted to extremely low concentrations (<0.12 nM) and resulted from the relatively high affinity used in the model for bacteria ($0.5\,l\,n\,mol^{-1}\,l^{-1}$) and phytoplankton ($0.33\,l\,n\,mol^{-1}\,l^{-1}$) compared to in situ data (0.16 to $0.2\,l\,nmol\,h^{-1}$ (Moutin et al., 2002). To reduce the maximum affinity in our model, one could consider an increase of the half stauration constant (K_X), an increase in the minimum intracellular P content ($Q^P_{\min}$) or a decrease in the maximum uptake rate $V_X^{\max}$. Yet, any modification of these parameters will be constrained by size considerations since increasing P requirement will increase the amount of phosphorus per unit of cell volume and decreasing $V^{\max}$ or increasing K will imply a smaller size (Eq. 22) which in turn induces an increase in element concentrations per unit of cell volume. For nitrogen, the picture is more complicated, although phytoplanktonic cells display N-limitation for inorganic N concentrations below 2 nM, in the same environment, heterotrophic bacteria are C-limited. This feature is mainly the result of the strong coupling between nitrogen and carbon in phytoplanktonic cells which restricts the production of bioavailable carbon for heterotrophic bacteria under N-limited conditions. In general, the interaction between bacteria and phytoplankton from a carbon point of view is more complex than from a nutrient point of view. Quantitatively, model results are quite close to published data concerning the carbon dynamic in the Mediterranean sea. In the western basin, primary production rate range between 0.1 and $0.6\,\mu mol\,l^{-1}\,d^{-1}$ (Moutin and Raimbault, 2002; Lemee et al., 2002). Directly comparing in situ primary production with our model results is quite complicated since ^{14}C based primary production is neither a gross production rate nor a net production rate. In fact, Moutin et al. (1999)

BGD
7, 7091–7130, 2010

have proposed a model and estimated gross primary production to be:

$$GPP = 1.72 \ A_N^* \tag{28}$$

where A_N^* is the daily primary production (24 h dawn to dawn) rate measured with the ^{14}C method. With this approach, our gross primary production in the model is within the range of the previously cited studies. Concerning PER, the values displayed by the model may appear high, especially in extremely low P environment where it can reach up to 72% of GPP. The modelled values are much higher than the typical 16% of PER for the Mediterranean sea (Moran et al., 2002). On the other hand, in a control mesocosm environment using adriatic sea water, Fajon et al. (1999) reported values for PER as high as 80%. Thus it is difficult to assess to which extent our values of PER are unreasonable. In order to reduce the fraction of GPP exuded as PER, the quota function (Eq. 17) could be modify to:

$$f^{Q_X} = \left(\frac{Q_X^{\max} - Q_X}{Q_X^{\max} - Q_X^{\min}}\right)^n \tag{29}$$

Using n values lower than 1 in Eq. 29 would tend to decrease exudation rate when carbon content approaches $Q_C^{\min}$ but this in turn would decrease DOC availability for heterotrophic bacteria and may narrow the range of nutrient concentrations for which bacteria are nutrient limited. For this reason, and to avoid a loss of clarity in the model results due to the more complex form of the quota function, we did not include such description in the current model. Concerning the BP and BGE in the model, values are also quite close to expected values for the Mediterranean Sea. In the western basin, bacterial production range from 0.05 to 0.2 µmol l^{-1} d^{-1} (Wambeke et al., 2002; Lemee et al., 2002). Although BP measurements using the assimilation of radiolabbeled amino acids should be considered carefully when compared to model results, it seems that the model is relatively close to experimental values. In a review, del Giorgio and Cole (1998) estimated BGE to vary between less than 0.05 to as high as 0.6, with a systematic decrease with increasing oligotrophy. BGE in the model does decrease

BGD
7, 7091–7130, 2010

with decreasing nutrient availability and the range between 0.15 and 0.4 is reasonable given the large uncertainites associated with BGE measurements. From a more qualitative point of view, an interesting aspect of the model is its ability to reproduce the higher PER in P-limited system compared to N-limited system (Obernosterer and Herndl, 1995). This is a significant aspect that is not always taken into account when one wants to explain the particularly high DOC concentration in the surface layer of the Mediterranean sea. While some authors have suggested that P-limitation of heterotrophic bacteria could cause and accumulation of DOC during summer (Thingstad et al., 1997), other have used refractorization of DOC to explain the observed accumulation (Polimene et al., 2006) but differences may also arise from the producing end (Cauwet et al., 2002). We propose in this model a possible mechanism to explain the high DOC production under high N:P ratio. In our model, chlorophyll synthesis is not influenced by the P status of the cell but in contrast it is proportional to the N content of the phytoplankton cells. This was motivated by the fact that under N-limited environement authors have shown a bleaching of phytoplanktonic cells as a result of decreasing chlorophyll content (Schwarz and Forchhammer, 2005). High N:P environement combined with P-limitation of phytoplankton growth increase the uncoupling between GPP and growth and thus increase PER This implies a complex system where both source of bioavailable carbon (PER and mortality) display opposite trends. If we consider phytoplankton, when growth is severly limited by the availability of phosphate and when N is abundant, DOC production through exudation is maximum and represent almost all the carbon available for heteotrophic bacteria. When N and P are abundant DOC production through mortality increases with increasing growth rate but on the other hand, photosynthetic extracellular release decrease rapidly. It implies that heterotrophic bacteria may benefit from slow growing nutrient limited phytoplankton with high exudation rate, especially if we consider them more competitive for nutrients and if we assume PER to be a reliable source of DOC for heterotrophic bacteria. Another consequences is the more direct coupling between primary production and bacterial production under P-limited conditions, a feature that has been shown experimentally when comparing

BGD
7, 7091–7130, 2010

the eastern and the western basin (Turley et al., 2000).

Although model results could be improve especially concerning carbon dynamics, overall results are quite consistant with our current knowledge of the carbon cycle in the surface layer of the Mediterranean sea. In addition, our study of a steady state system gives us clear indication on the process that are responsible for the observed DOC accumulation in the surface layer of the Mediterranean Sea. First, based on the low value of DOC concentrations at steady state, our model suggest that DOC accumulation is probably not a continuous process and that during the stratified period, it is more likely that the system is balanced or net heterotrophic. However, the DOC accumulation observed under extremly low P concentrations suggest that the combination of high PER and P-limited growth may explain the high DOC concentration observed in the surface layer of the Mediterranean sea during summer. High PER could arise due to the unusual N:P ratio found in the Mediterranean Sea (Krom et al., 1992). The fact that DOC concentrations at surface of the ocean increases between the Atlantic ocean and the western mediterranean basin (Aminot and Kerouel, 2004) and between the western and the eastern mediterranean basin (Pujo-Pay et al., 2010); and the fact that along the same transect, the N:P ratio increases from 16:1 for the Atlantic ocean to more than 28:1 for the eastern mediterranean basin (Pujo-Pay, 2010), may suggest that the observed role of the N:P ratio on DOC accumulation in the model is somehow representative of what is occuring on seasonal time scales (eventhough our model intend to represent mechanisms occuring on shorter time scales). In fact, one should keep in mind that the trend we have described here would be even more pronounced if one takes into account the uncoupling of bacterial and phytoplanktonic biomass during the spring bloom, due to stronger grazing pressure on heterotrophic bacteria. In other word, DOC accumulation in our simulations would be much greater if bacterial cell number is kept constant while phytoplankton cell number goes up.

BGD
7, 7091–7130, 2010

6 Conclusions

In our study, we focused on the surface layer of the Mediterranean Sea. In summer, this system is characterized by low nutrient concentrations, realtively stable populations of phytoplankton and heterotrophic bacteria and high DOC concentrations. the interaction between phytoplankton and heterotrophic bacteria is characterized by strong competitions for nutrients and commensalism for carbon. To better understand the balance between growth and carbon production/consumption, we implemented in Eco3M a multi-element, mechanistic steady state model with cell abundances as an explicit variable. With this model, we studied the different steady state results obtained under various amount of inorganic nitrogen and phosphate. We verified that the magnitude of the the different stocks and fluxes displayed by the model were in aggreement with the in situ data found in the litterature for the Mediterranean Sea. This approach allows us to determine the conditions for wich osmotrophs may be nutrient limited rather than energy (carbon) limited. In addition, the model gave us insight on the primary production rate, DOC exudation and bacterial growth efficiency necessary to maintain a steady state regime and highlighted the need for more accurate estimates of these parameters. Last but not least, the model displayed significant differences between N and P limited systems and we used this results to explain why DOC accumulation in the surface layer of the ocean may be a characterisitic of P-limited systems and how the balance between chlorophyll production and growth could explain the high exudation rate observed under low P and high N environment.

Acknowledgements. This is a contribution of the BOUM (Biogeochemistry from the Oligotrophic to the Ultraoligotrophic Mediterranean) experiment (http://www.com.univ-mrs.fr/BOUM) of the french national LEFE-CYBER program, the european IP SESAME and the international IMBER project. The BOUM experiment was coordinated by the Institut des Sciences de l'Univers (INSU) and managed by the Centre National de la Recherche Scientifique (CNRS).

BGD
7, 7091–7130, 2010

The publication of this article is financed by CNRS-INSU.

References

Aminot, A. and Kerouel, R.: Dissolved organic carbon, nitrogen and phosphorus in the N-E Atlantic and the N-W Mediterranean with particular reference to non-refractory fractions and degradation, Deep-Sea Res. Pt. I, 51, 1975–1999, 2004. 7111

Anderson, T. R. and Ducklow, H. W.: Microbial loop carbon cycling in ocean environments studied using a simple steady-state model, Aquat. Microb. Ecol., 26, 37–49, 2001. 7106

Anderson, T. R. and Turley, C. M.: Low bacterial growth efficiency in the oligotrophic eastern Mediterranean Sea: a modelling analysis, J. Plankton Res., 25, 1011–1019, 2003. 7106

Baklouti, M., Diaz, F., Pinazo, C., Faure, V., and Quguiner, B.: Investigation of mechanistic formulations depicting phytoplankton dynamics for models of marine pelagic ecosystems and description of a new model, Prog. Oceanogr., 71, 1–33, 2006a. 7100

Baklouti, M., Faure, V., Pawlowski, L., and Sciandra, A.: Investigation and sensitivity analysis of a mechanistic phytoplankton model implemented in a new modular numerical tool (Eco3M) dedicated to biogeochemical modelling, Prog. Oceanogr., 71, 34–58, 2006b. 7100

Bertilsson, S., Berglund, O., Karl, D. M., and Chisholm, S. W.: Elemental composition of marine Prochlorococcus and Synechococcus: Implications for the ecological stoichiometry of the sea, Limnol. Oceanogr., 48, 1721–1731, 2003. 7097

Cauwet, G., Deliat, G., Krastev, A., Shtereva, G., Becquevort, S., Lancelot, C., Momzikoff, A., Saliot, A., Cociasu, A., and Popa, L.: Seasonal DOC accumulation in the Black Sea: a regional explanation for a general mechanism, Mar. Chem., 79, 193–205, 2002. 7110

Christaki, U., Giannakourou, A., Van Wambeke, F., and Gregori, G.: Nanoflagellate predation on auto- and heterotrophic picoplankton in the oligotrophic Mediterranean Sea, J. Plankton Res., 23, 1297–1310, 2001. 7094

Christaki, U., Courties, C., Karayanni, H., Giannakourou, A., Maravelias, C., Kormas, K. A., and Lebaron, P.: Dynamic characteristics of Prochlorococcus and Synechococcus consumption by bacterivorous nanoflagellates, Microb. Ecol., 43, 341–352, 2002. 7102

Claustre, H., Babin, M., Merien, D., Ras, J., Prieur, L., Dallot, S., Prasil, O., Dousova, H., and Moutin, T.: Toward a taxon-specific parameterization of bio-optical models of primary production: A case study in the North Atlantic, J. Geophys. Res., 110, C07S12, doi:10.1029/2004JC002634, 2005. 7101

del Giorgio, P. A. and Cole, J. J.: Bacterial Growth Efficiency in Natural Aquatic Systems, Ann. Rev. Ecol. Syst., 29, 503–541, 1998. 7109

Diaz, F. and Raimbault, P.: Nitrogen regeneration and dissolved organic nitrogen release during spring in a NW Mediterranean coastal zone (Gulf of Lions): implications for the estimation of new production, Mar. Ecol.-Prog. Ser., 197, 51–65, 2000. 7107

Droop, M. R.: Vitamin B12 and Marine Ecology. IV. The Kinetics of Uptake, Growth and Inhibition in Monochrysis Lutheri, J. Mar. Biol. Assoc. UK, 48, 689–733, 1968. 7096

Duhamel, S., Moutin, T., Van Wambeke, F., Van Mooy, B., Rimmelin, P., Raimbault, P., and Claustre, H.: Growth and specific P-uptake rates of bacterial and phytoplanktonic communities in the Southeast Pacific (BIOSOPE cruise), Biogeosciences, 4, 941–956, doi:10.5194/bg-4-941-2007, 2007. 7107

Fagerbakke, K. M., Heldal, M., and Norland, S.: Content of carbon, nitrogen, oxygen, sulfur and phosphorus in native aquatic and cultured bacteria, Aquat. Microb. Ecol., 10, 15–27, 1996. 7097

Fajon, C., Cauwet, G., Lebaron, P., Terzic, S., Ahel, M., Malej, A., Mozetic, P., and Turk, V.: The accumulation and release of polysaccharides by planktonic cells and the subsequent bacterial response during a controlled experiment, Fems Microbiol. Ecol., 29, 351–363, 1999. 7109

Fu, F. X., Zhang, Y. H., Feng, Y. Y., and Hutchins, D. A.: Phosphate and ATP uptake and growth kinetics in axenic cultures of the cyanobacterium Synechococcus CCMP 1334, Eur. J. Phycol., 41, 15–28, 2006. 7099

Fukuda, R., Ogawa, H., Nagata, T., and Koike, I.: Direct determination of carbon and nitrogen contents of natural bacterial assemblages in marine environments, Appl. Environ. Microbiol., 64, 3352–3358, 1998. 7097

Goldman, J. and McCarthy, J.: Steady State Growth and Ammonium Uptake of a Fast-Growing Marine Diatom, Limnol. Oceanogr., 23, 695–703, 1978. 7097

BGD
7, 7091–7130, 2010

Gundersen, K., Heldal, M., Norland, S., Purdie, D. A., and Knap, A. H.: Elemental C, N, and P cell content of individual bacteria collected at the Bermuda Atlantic Time-Series Study (BATS) site, Limnol. Oceanogr., 47, 1525–1530, 2002. 7097

Hagstrom, A., Azam, F., Andersson, A., Wikner, J., and Rassoulzadegan, F.: Microbial Loop In An Oligotrophic Pelagic Marine Ecosystem – Possible Roles Of Cyanobacteria And Nanoflagellates In The Organic Fluxes, Mar. Ecol.-Prog. Ser., 49, 171–178, 1988. 7094

Han, B.-P.: A Mechanistic Model of Algal Photoinhibition Induced by Photodamage to Photosystem-II, J. Theor. Biol., 214, 519–527, 2002. 7100

Healey, F. P.: Slope of the Monod equation as an indicator of advantage in nutrient competition, Microb. Ecol., 5, 281–286, 1980. 7099

Heldal, M., Scanlan, D. J., Norland, S., Thingstad, F., and Mann, N. H.: Elemental composition of single cells of various strains of marine Prochlorococcus and Synechococcus using X-ray microanalysis, Limnol. Oceanogr., 48, 1732–1743, 2003. 7097

Ikeya, T., Ohki, K., Takahashi, M., and Fujita, Y.: Study on phosphate uptake of the marine cyanophyte Synechococcus sp NIBB 1071 in relation to oligotrophic environments in the open ocean, Mar. Biol., 129, 195–202, 1997. 7097, 7099

Klausmeier, C., Litchman, E., Daufresne, T., and Levin, S.: Phytoplankton stoichiometry, Ecol. Res., 23, 479–485, 2008. 7096

Krom, M. D., Kress, N., Brenner, S., and Gordon, L. I.: Phosphorus Limitation of Primary Productivity in the Eastern Mediterranean Sea, Limnol. Oceanogr., 36, 424–432, 1991. 7092

Krom, M. D., Brenner, S., Kress, N., Neori, A., and Gordon, L. I.: Nutrient Dynamics And New Production In A Warm-Core Eddy From The Eastern Mediterranean-Sea, Deep-Sea Res., 39, 467–480, 1992. 7107, 7111

Lehman, J., Daniel B. Botkin, D., and Likens, G.: The Assumptions and Rationales of a Computer Model of Phytoplankton Population Dynamics, Limnol. Oceanogr., 20, 343–364, 1975. 7098

Lemee, R., Rochelle-Newall, E., Van Wambeke, F., Pizay, M. D., Rinaldi, P., and Gattuso, J. P.: Seasonal variation of bacterial production, respiration and growth efficiency in the open NW Mediterranean Sea, Aquat. Microb. Ecol., 29, 227–237, 2002. 7102, 7108, 7109

Lovdal, T., Skjoldal, E. F., Heldal, M., Norland, S., and Thingstad, T. F.: Changes in morphology and elemental composition of Vibrio splendidus along a gradient from carbon-limited to phosphate-limited growth, Microb. Ecol., 55, 152–161, 2008. 7097

Magazzu, G. and Decembrini, F.: Primary production, biomass and abundance of phototrophic

BGD
7, 7091–7130, 2010

picoplankton in the Mediterranean Sea: a review, Aquat. Microb. Ecol., 09, 97–104, 1995. 7094
Maranon, E.: Phytoplankton growth rates in the Atlantic subtropical gyres, Limnol. Oceanogr., 50, 299–310, 2005. 7107
Middelboe, M. and Sondergaard, M.: Bacterioplankton Growth Yield: Seasonal Variations and Coupling to Substrate Lability and beta-Glucosidase Activity, Appl. Environ. Microbiol., 59, 3916–3921, 1993. 7100
Moran, X. A. G., Estrada, M., Gasol, J. M., and Pedros-Alio, C.: Dissolved primary production and the strength of phytoplankton bacterioplankton coupling in contrasting marine regions, Microb. Ecol., 44, 217–223, 2002. 7109
Moutin, T. and Raimbault, P.: Primary production, carbon export and nutrients availability in western and eastern Mediterranean Sea in early summer 1996 (MINOS cruise), J. Marine Syst., 33–34, 273–288, 2002. 7094, 7108
Moutin, T., Raimbault, P., and Poggiale, J.-C.: Primary production in surface waters of the western Mediterranean sea. Calculation of daily production, Comptes Rendus de l'Acadmie des Sciences – Series III – Sciences de la Vie, 322, 651–659, 1999. 7108
Moutin, T., Thingstad, T. F., Van Wambeke, F., Marie, D., Slawyk, G., Raimbault, P., and Claustre, H.: Does competition for nanomolar phosphate supply explain the predominance of the cyanobacterium Synechococcus?, Limnol. Oceanogr., 47, 1562–1567, 2002. 7107, 7108
Moutin, T., Karl, D. M., Duhamel, S., Rimmelin, P., Raimbault, P., Van Mooy, B. A. S., and Claustre, H.: Phosphate availability and the ultimate control of new nitrogen input by nitrogen fixation in the tropical Pacific Ocean, Biogeosciences, 5, 95–109, doi:10.5194/bg-5-95-2008, 2008. 7092
Obernosterer, I. and Herndl, G. J.: Phytoplankton Extracellular Release And Bacterial-Growth – Dependence On The Inorganic N-P Ratio, Mar. Ecol.-Prog. Ser., 116, 247–257, 1995. 7110
Polimene, L., Allen, J. I., and Zavatarelli, M.: Model of interactions between dissolved organic carbon and bacteria in marine systems, Aquat. Microb. Ecol., 43, 127–138, 2006. 7110
Robarts, R. D., Zohary, T., Waiser, M. J., and Yacobi, Y. Z.: Bacterial abundance, biomass, and production in relation to phytoplankton biomass in the Levantine Basin of the southeastern Mediterranean Sea, Mar. Ecol.-Prog. Ser., 137, 273–281, 1996. 7102
Schwarz, R. and Forchhammer, K.: Acclimation of unicellular cyanobacteria to macronutrient deficiency: emergence of a complex network of cellular responses, Microbiol.-Sgm, 151, 2503–2514, 2005. 7110

BGD
7, 7091–7130, 2010

Siokou-Frangou, I., Christaki, U., Mazzocchi, M. G., Montresor, M., Ribera d'Alcalá, M., Vaqué, D., and Zingone, A.: Plankton in the open Mediterranean Sea: a review, Biogeosciences, 7, 1543–1586, doi:10.5194/bg-7-1543-2010, 2010. 7102

Sondergaard, M. and Middelboe, M.: A Cross-System Analysis Of Labile Dissolved Organic-Carbon, Mar. Ecol.-Prog. Ser., 118, 283–294, 1995. 7094

Tanaka, T. and Rassoulzadegan, F.: Full-depth profile (0-2000 m) of bacteria, heterotrophic nanoflagellates and ciliates in the NW Mediterranean Sea: Vertical partitioning of microbial trophic structures, Deep-Sea Res. Pt. II, 49, 2093–2107, 2002. 7102

Tanaka, T. and Rassoulzadegan, F.: Vertical and seasonal variations of bacterial abundance and production in the mesopelagic layer of the NW Mediterranean Sea: bottom-up and top-down controls, Deep-Sea Res. Pt. I, 51, 531–544, 2004. 7102

Terry, K. L., Laws, E. A., and Burns, D. J.: Growth-Rate Variation In The N-P Requirement Ratio Of Phytoplankton, J. Phycol., 21, 323–329, 1985. 7097

Thingstad, T.: Simulating the response to phosphate additions in the oligotrophic eastern Mediterranean using an idealized four-member microbial food web model, Deep Sea Res. Pt. II, 52, 3074–3089, 2005. 7093, 7106

Thingstad, T. and Lignell, R.: Theoretical models for the control of bacterial growth rate, abundance, diversity and carbon demand, Aquat. Microb. Ecol., 13, 19–27, 1997. 7101

Thingstad, T. F.: Utilization Of N, P, And Organic C By Heterotrophic Bacteria. 1. Outline Of A Chemostat Theory With A Consistent Concept Of Maintenance Metabolism, Mar. Ecol.-Prog. Ser., 35, 99–109, 1987. 7101

Thingstad, T. F. and Rassoulzadegan, F.: Conceptual models for the biogeochemical role of the photic zone microbial food web, with particular reference to the Mediterranean Sea, Prog. Oceanogr., 44, 271–286, 1999. 7098

Thingstad, T. F., Dolan, J. R., and Fuhrman, J. A.: Loss rate of an oligotrophic bacterial assemblage as measured by H-3-thymidine and (PO4)-P-32: Good agreement and near-balance with production, Aquat. Microb. Ecol., 10, 29–36, 1996. 7107

Thingstad, T. F., Hagstrom, A., and Rassoulzadegan, F.: Accumulation of degradable DOC in surface waters: Is it caused by a malfunctioning microbial loop?, Limnol. Oceanogr., 42, 398–404, 1997. 7106, 7110

Thingstad, T. F., Zweifel, U. L., and Rassoulzadegan, F.: P limitation of heterotrophic bacteria and phytoplankton in the northwest Mediterranean, Limnol. Oceanogr., 43, 88–94, 1998. 7092, 7108

BGD
7, 7091–7130, 2010

Thingstad, T. F., Krom, M. D., Mantoura, R. F. C., Flaten, G. A. F., Groom, S., Herut, B., Kress, N., Law, C. S., Pasternak, A., Pitta, P., Psarra, S., Rassoulzadegan, F., Tanaka, T., Tselepides, A., Wassmann, P., Woodward, E. M. S., Riser, C. W., Zodiatis, G., and Zohary, T.: Nature of Phosphorus Limitation in the Ultraoligotrophic Eastern Mediterranean, Science, 309, 1068–1071, 2005. 7092, 7108

Turley, C. M., Bianchi, M., Christaki, U., Conan, P., Harris, J. R. W., Psarra, S., Ruddy, G., Stutt, E. D., Tselepides, A., and Van Wambeke, F.: Relationship between primary producers and bacteria in an oligotrophic sea - the Mediterranean and biogeochemical implications, Mar. Ecol.-Prog. Ser., 193, 11–18, 2000. 7111

Vadstein, O. and Olsen, Y.: Chemical-Composition And Phosphate-Uptake Kinetics Of Limnetic Bacterial Communities Cultured In Chemostats Under Phosphorus Limitation, Limnol. Oceanogr., 34, 939–946, 1989. 7099

Vaulot, D., LeBot, N., Marie, D., and Fukai, E.: Effect of Phosphorus on the Synechococcus Cell Cycle in Surface Mediterranean Waters during Summer, Appl. Environ. Microbiol., 62, 2527–2533, 1996. 7096

Wambeke, F., Goutx, M., Striby, L., Sempere, R., and Vidussi, F.: Bacterial dynamics during the transition from spring bloom to oligotrophy in the northwestern Mediterranean Sea: relationships with particulate detritus and dissolved organic matter, Mar. Ecol.Prog. Ser., 212, 89–105, 2001. 7102

Wambeke, F., Christaki, U., Giannakourou, A., Moutin, T., and Souvemerzoglou, K.: Longitudinal and Vertical Trends of Bacterial Limitation by Phosphorus and Carbon in the Mediterranean Sea, Microb. Ecol., 43, 119–133, 2002. 7093, 7108, 7109

Weger, H. G., Herzig, R., Falkowski, P. G., and Turpin, D. H.: Respiratory Losses In The Light In A Marine Diatom - Measurements By Short-Term Mass-Spectrometry, Limnol. Oceanogr., 34, 1153–1161, 1989. 7101

Yentsch, C. and Vaccaro, R.: Phytoplankton Nitrogen in the Oceans, Limnol. Oceanogr., 3, 443–448, 1958. 7101

Yuan-Hui, L. and Gregory, S.: Diffusion of ions in sea water and in deep-sea sediments, Geochim. Cosmochim. Ac., 38, 703–714, 1974. 7099

BGD
7, 7091–7130, 2010

Table 1. Model's state variables.

Symbol	Definition	Unit
ϕ	Phytoplankton abundance	cell m^{-3}
ϕ_C	Phytoplankton carbon biomass	mol m^{-3}
ϕ_N	Phytoplankton nitrogen biomass	mol m^{-3}
ϕ_P	Phytoplankton phosphate biomass	mol $m4^{-3}$
ϕ_{Chl}	Phytoplankton Chlorophyll biomass	g m^{-3}
β	Bacteria abundance	cell m^{-3}
β_C	Bacteria carbon biomass	mol m^{-3}
β_N	Bacteria nitrogen biomass	mol m^{-3}
β_P	Bacteria phosphate biomass	mol m^{-3}
LDOC	Labile DOC concentration	mol m^{-3}
SLDOC	Semi-labile DOC concentration (PER)	mol m^{-3}
SRDOC	Semi-refractory DOC concentration	mol m^{-3}
N	Inorganic nitrogen concentration	mol m^{-3}
P	Inorganic phosphate concentration	mol m^{-3}

BGD
7, 7091–7130, 2010

Table 2. Elemental content and growth parameters.

Symbol	Definition	Unit	Phytoplankton	Bacteria
Q_X	Organism cell quota for the element X	mol cell^{-1}	$\frac{\phi_X}{\phi}$	$\frac{\beta_X}{\beta}$
Elemental Content				
Q_P^{min}	minimum phosphate content	fmol cell^{-1}	0.06	0.016
Q_P^{max}	maximum phosphate content	fmol cell^{-1}	$2.5\,Q_P^{min}$	
Q_N^{min}	minimum nitrogen content	fmol cell^{-1}	$16\,Q_P^{min}$	$10\,Q_P^{min}$
Q_N^{max}	maximum nitrogen content	fmol cell^{-1}	$2.5\,Q_N^{min}$	
Q_C^{min}	minimum carbon content	fmol cell^{-1}	$106\,Q_P^{min}$	$50\,Q_P^{min}$
Q_C^{max}	maximum carbon content	fmol cell^{-1}	$2.5\,Q_C^{min}$	
Growth				
$\bar{\mu}$	maximum cellular growth rate	d^{-1}	2	

BGD
7, 7091–7130, 2010

Table 3. Uptake parameters.

Symbol	Definition		Unit	Values ϕ	Values β
D	Molecular diffusion rate		$m^2\ s^{-1}$	$1\ 10^{-9}$	
r	Cell radius		µm	0.5	0.18
α_P	Affinity for phosphate	$\frac{4\pi D r}{Q_P^{min}}$	$l\ nmol\ h^{-1}$	0.33	0.5
α_N	Affinty for nitrogen	$\frac{4\pi D r}{Q_N^{min}}$	$l\ nmol\ h^{-1}$	0.021	0.05
V_P^{max}	Maximum phosphate uptake rate		$fmol\ cell^{-1}\ h^{-1}$	2.16	0.32
V_N^{max}	Maximum nitrogen uptake rate		$fmol\ cell^{-1}\ h^{-1}$	V_P^{max}	
V_{LDOC}^{max}	Maximum LDOC uptake rate		$fmol\ cell^{-1}\ h^{-1}$	–	0.18
V_{SLDOC}^{max}	Maximum SLDOC uptake rate		$fmol\ cell^{-1}\ h^{-1}$	–	$\frac{V_{LDOC}^{max}}{2}$
V_{SRDOC}^{max}	Maximum SRDOC uptake rate		$fmol\ cell^{-1}\ h^{-1}$	–	V_{SLDOC}^{max}
K_P	Half-saturation constant for phosphate		nM	100	40
K_N	Half-saturation constant for nitrogen		nM	K_P	
K_{LDOC}	Half-saturation constant for LDOC		nM	–	K_P
K_{SLDOC}	Half-saturation constant for SLDOC		nM	–	100
K_{SRDOC}	Half-saturation constant for SRDOC		nM	–	K_{SLDOC}

BGD
7, 7091–7130, 2010

Table 4. Photosynthesis and chlorophyll parameters.

Symbol	Definition	Unit	Phytoplankton
τ	Electron turnover-time in PSII	s	$2.5\,10^{-3}$
σ_{PSII}	PSII cross section	$m^2\,J^{-1}$	8
k_d^H	Dimensionless rate of PSII damage	–	$4.5\,10^{-8}$
k_r	PSII repair rate	s^{-1}	$2.6\,10^{-4}$
$\bar{a}^*$	Mean Chla-specific absorption coefficient	$m^2\,gChl_a^{-1}$	37
ϕ^C_{max}	Maximum quantum yield for carbon fixation	$molC\,J^{-1}$	$1\,10^{-7}$
$Q^{max}_{Chl/N}$	Maximum chlorophyll to nitrogen ratio	$g\,Chl\,mol\,N^{-1}$	2

BGD
7, 7091–7130, 2010

Table 5. Respiration parameters.

Symbol	Definition	Unit	Values
ω_1	Efficiency of LDOC uptake	–	0.7
ω_2	Efficiency of SLDOC uptake	–	0.5
ω_3	Efficiency of SRDOC uptake	–	0.3
ω_4	Fraction of surplus C respired	s^{-1}	$2.89\,10^{-5}$

BGD
7, 7091–7130, 2010

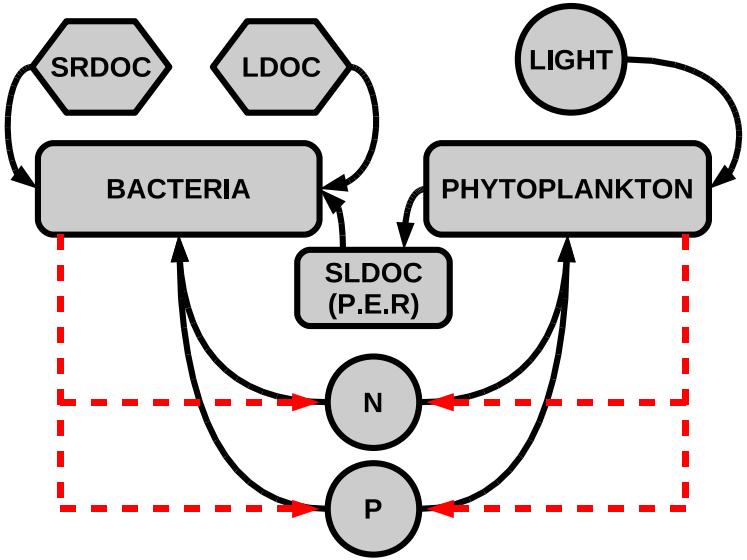

Fig. 1. Diagram representing a simplified system of competition and commensalism between bacteria and phytoplankton. Both groups are competing for nutrients (N, P) but while phytoplankton relies on light to produce carbon, bacteria uses three organic carbon sources that originated either from photosynthetic extracellular release (PER) or from grazing and mortality. PER was considered a semi-labile DOC source (SLDOC). 40% of DOC from grazing and mortality was considered semi-refractory (SRDOC) and 10% was considered as labile (LDOC).

BGD
7, 7091–7130, 2010

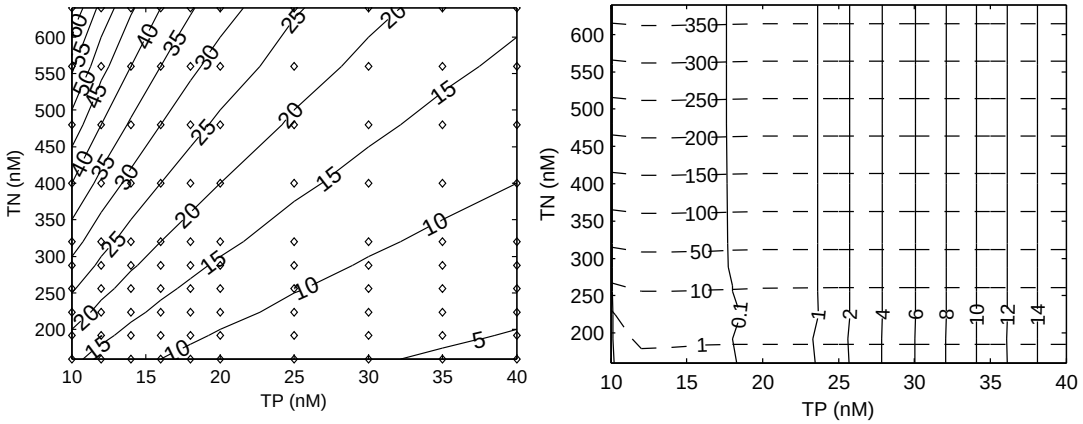

(a) Range of TN and TP used in this study

(b) Nutrient concentrations at steady state in nM

Fig. 2. **(a)** Range of total nitrogen (TN) and total phosphate (TP) concentrations tested with the model (isolines represent the TN to TP ratio and diamonds markers represent the different simulations). **(b)** Inorganic nutrient concentrations at steady state in nM as a function of TN and TP (dashed lines represent inorganic nitrogen and solid lines inorganic phosphate).

BGD
7, 7091–7130, 2010

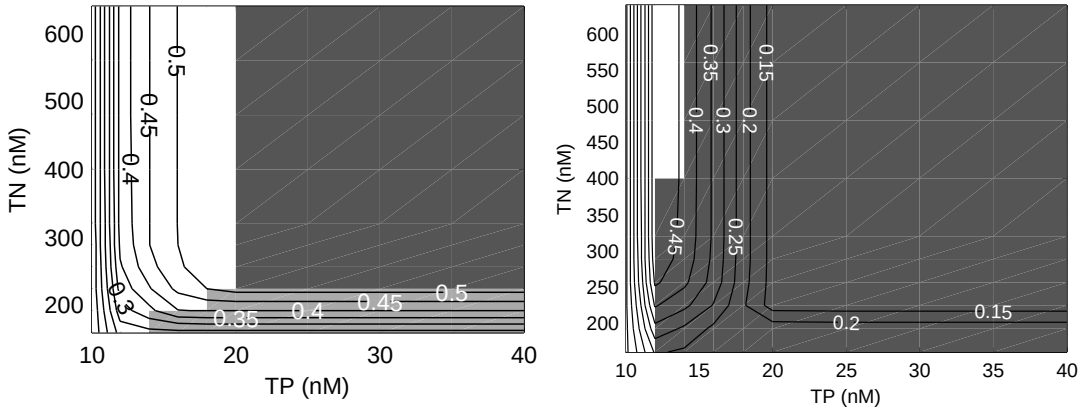

(a) Phytoplankton growth rate (d^{-1})

(b) Bacterial growth rate (d^{-1})

Fig. 3. Phytoplankton and bacterial growth rates per day as a function of total nitrogen (TN) and total phosphate (TP). Background color represents the element which is most limiting growth (white color represents P-limitation, light gray, N-limitation and dark gray C-limitation).

BGD
7, 7091–7130, 2010

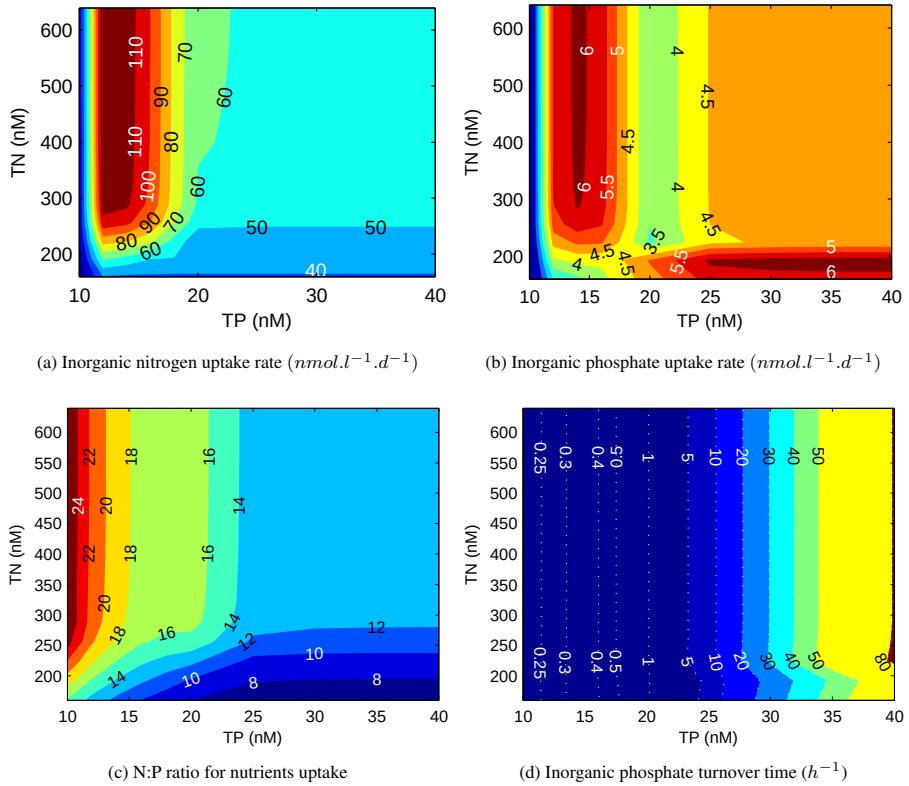

Fig. 4. Inorganic N **(a)** and P **(b)** uptake rate (nmol l^{-1} d^{-1}), **(c)** N to P ratio of nutrient uptake and **(d)** inorganic phosphate turnover time (h^{-1}) as a function of TN and TP.

BGD
7, 7091–7130, 2010

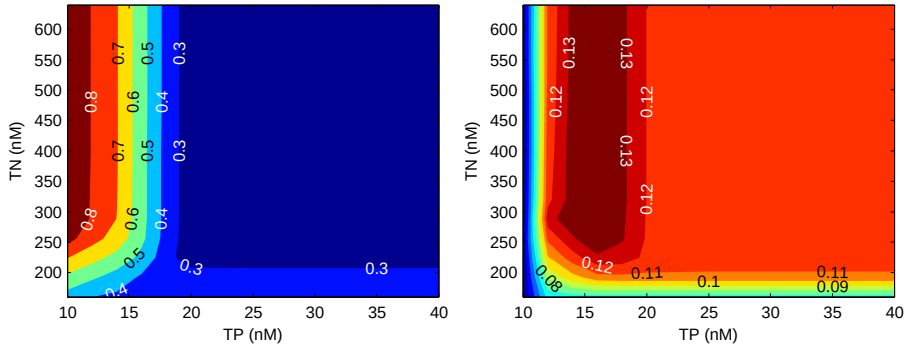

(a) Gross primary production ($\mu mol.l^{-1}.d^{-1}$)

(b) Net primary production ($\mu mol.l^{-1}.d^{-1}$)

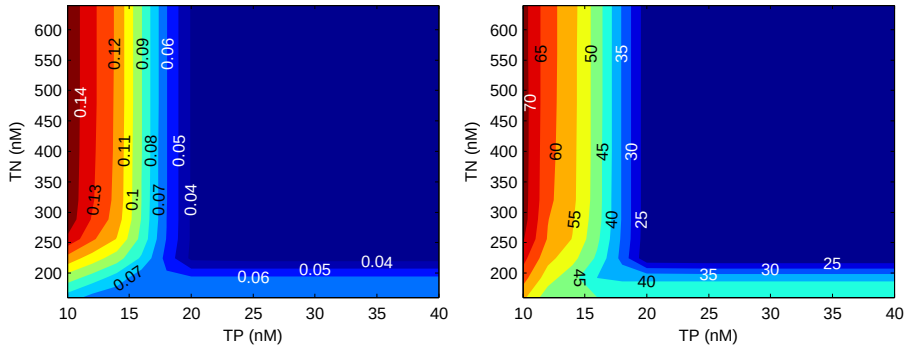

(c) Chlorophyll ($\mu g.l^{-1}$)

(d) Photosynthetic extracellular release (% GPP)

Fig. 5. Gross primary production (GPP), Net primary production (NPP), Chlorophyll concentration and photosynthetic extracellular released (PER) as a function of TN and TP.

BGD
7, 7091–7130, 2010

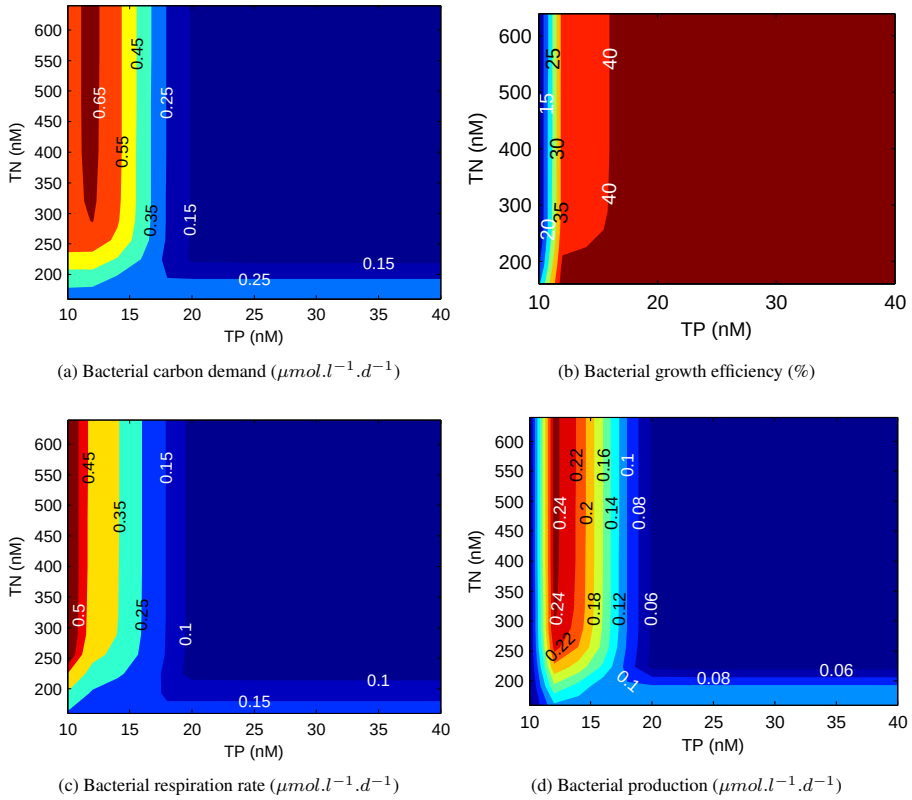

(a) Bacterial carbon demand ($\mu mol.l^{-1}.d^{-1}$)

(b) Bacterial growth efficiency (%)

(c) Bacterial respiration rate ($\mu mol.l^{-1}.d^{-1}$)

(d) Bacterial production ($\mu mol.l^{-1}.d^{-1}$)

Fig. 6. Bacterial carbon demand (BCD), bacterial growth efficiency (BGE), Bacterial respiration rate (BR) and Bacterial production (BP) as a function of TN and TP.

BGD
7, 7091–7130, 2010

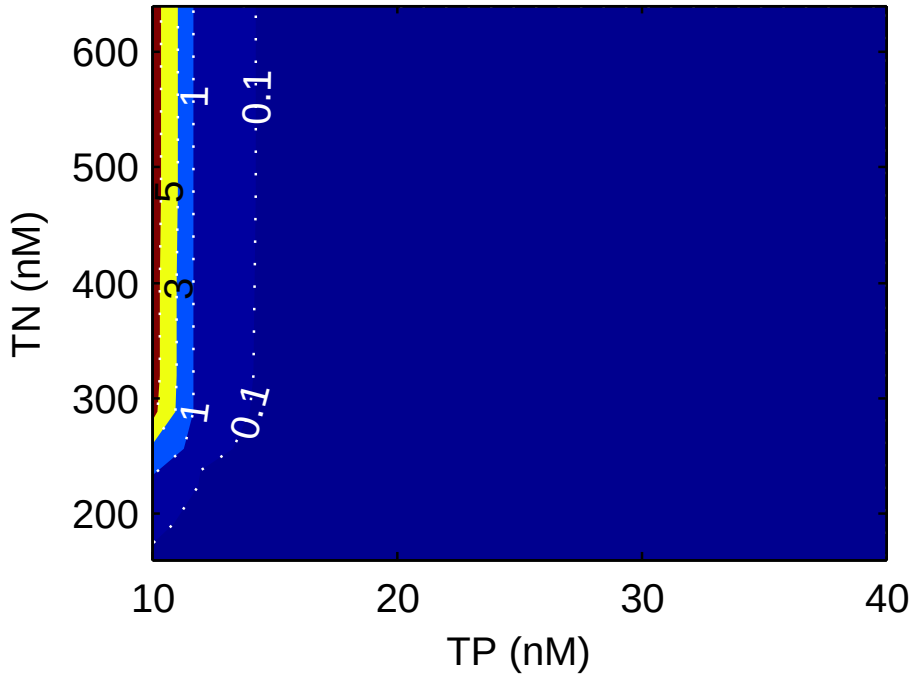

Fig. 7. Dissolved organic carbon concentrations in μM after 100 days of simulation as a function of TN and TP.

BGD
7, 7091–7130, 2010